



HCl ppb-level detection based on QEPAS sensor using a low resonance frequency quartz tuning fork



Yufei Ma ^{a,b,*}, Ying He ^a, Xin Yu ^a, Cheng Chen ^a, Rui Sun ^c, Frank K. Tittel ^b

^a National Key Laboratory of Science and Technology on Tunable Laser, Harbin Institute of Technology, Harbin 150001, China

^b Department of Electrical and Computer Engineering, Rice University, 6100 Main Street, Houston, TX 77005, USA

^c Post-doctoral Mobile Station of Power Engineering and Engineering Thermophysics, Harbin Institute of Technology, Harbin 150001, China

ARTICLE INFO

Article history:

Received 14 January 2016

Received in revised form 18 April 2016

Accepted 19 April 2016

Available online 20 April 2016

Keywords:

Trace gas detection

QEPAS

Hydrogen chloride (HCl)

Quartz tuning fork

ABSTRACT

In this report, a sensitive quartz-enhanced photoacoustic spectroscopy (QEPAS) based hydrogen chloride (HCl) sensor using a quartz tuning fork (QTF) with a resonance frequency of 30.72 kHz was demonstrated for the first time. A fiber-coupled, continuous wave (CW), distributed feedback (DFB) diode laser emitting at 1.74 μm was employed as the excitation laser source. Wavelength modulation spectroscopy and a 2nd harmonic detection technique were used to reduce the sensor background noise. An acoustic micro-resonator (mR) was added to the QTF sensor architecture to improve the signal amplitude. For the reported HCl sensor system operating at atmospheric pressure, a 550 ppbv (parts per billion by volume) minimum detection limit at 5739.27 cm⁻¹ was achieved when the modulation depth and the data acquisition time were set to 0.23 cm⁻¹ and 1 s, respectively. The ppb-level detection sensitivity and robust design of the QEPAS technique makes it suitable for use in environmental monitoring and other applications.

© 2016 Elsevier B.V. All rights reserved.

1. Introduction

Hydrogen chloride (HCl), a toxic gas, is primarily produced by burning fuels that contain chlorine and incinerating waste that contains plastics [1,2]. HCl is not only a source of dioxin and acid rain, but also has been identified as hazardous in industrial workplaces, with a short period exposure limit of 5 ppm. Furthermore, HCl has performed an important role in photochemistry [3] and plasma etching [4]. Hence, there is a significant need for sensitive detection of HCl gas concentrations at sub-ppm levels.

Laser absorption spectroscopy (LAS) has the advantages that include fast response, non-invasive, highly sensitive and selective detection compared with chemical sensors which are currently widely used for HCl detection [5]. Tunable diode laser absorption spectroscopy (TDLAS) was adopted for HCl measurements [4,6] and a minimum detection limit (MDL) of 45 ppm was obtained [6]. In order to further improve the detection sensitivity, a multi-pass gas cell (MPGC) is usually used in the TDLAS technique, where the effective optical path length is typically tens and even hundreds of meters in order to reach a detection limit of the analyte trace gas species at ppb concentration levels [7–9]. However for ultra-high sensitive measurements these sensors are usually bulky and costly

due to the large size of a MPGC and the increased number of optical components that are needed for laser beam alignment and detection. Photoacoustic spectroscopy (PAS) is another effective trace gas sensor technology which employs a broadband microphone for acoustic wave detection. When the output of a near-infrared semiconductor laser is absorbed by a gas sample, the absorbed energy is transformed to heat energy by non-radiative processes, and will subsequently result in an increase of the local temperature and pressure in the sample. Therefore the absorption of a modulated near-infrared laser beam in a gas sample leads to the generation of an acoustic wave. The intensity of the acoustic wave is related to the sample concentration which can be detected by a sensitive microphone. However, most microphone-based PAS cells have a low resonance frequency (<2 kHz), which makes such cells more sensitive to environmental and sample gas flow noise [10].

A modification of the conventional PAS is the quartz-enhanced photoacoustic spectroscopy (QEPAS) technique which was first reported in 2002 [11]. This technique uses a commercially available millimeter sized piezoelectric quartz tuning fork (QTF) as an acoustic wave transducer. The high Q-factor and narrow resonance frequency band of QTF improve the QEPAS selectivity and immunity to environmental acoustic noise. The primary noise source of

* Corresponding author.

E-mail address: mayufei926@163.com (Y. Ma).

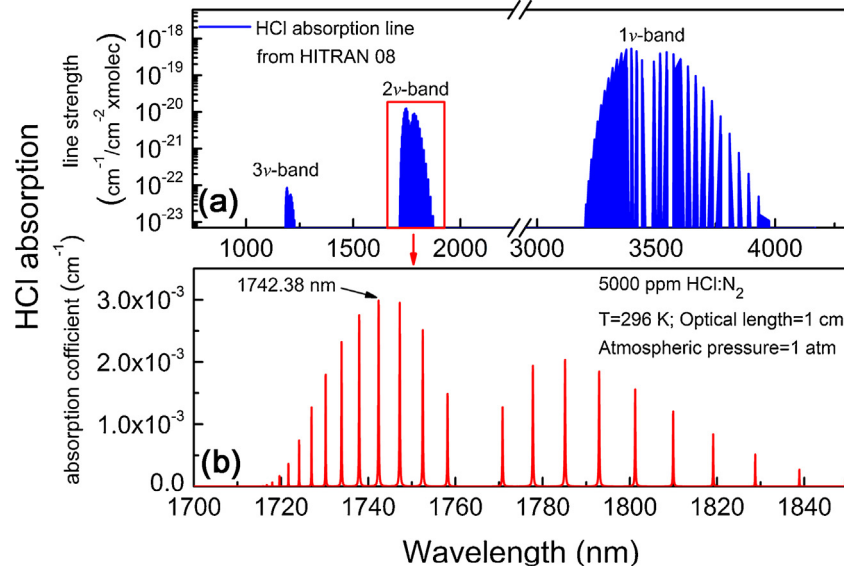


Fig. 1. HITRAN based simulation of HCl absorption spectra: (a) absorption line strength; (b) absorption coefficient at 296 K, standard atmospheric pressure, and an optical path length of 1 cm for 5000 ppm HCl:N₂.

QEPAS is limited by the fundamental Johnson thermal noise of the QTF. The QEPAS signal amplitude S is given by equation (1) [12].

$$S \propto \frac{\alpha P Q}{f_0} \quad (1)$$

where α is the absorption coefficient, P is the optical power, Q is the Q-factor of QTF, f_0 is the resonance frequency of QTF. From Eq. (1) it is seen that the QEPAS signal amplitude S is inversely proportional to the QTF resonance frequency. This is due to the fact that a QTF with a smaller f_0 will result in a longer effective integration time, which increases the QEPAS signal. In QEPAS, commercially available QTFs with a f_0 of ~ 32.76 kHz are usually employed, and only since 2013 the use of custom QTFs in QEPAS based sensor systems were reported [13–15].

In this paper, a high sensitive HCl trace gas sensor based on QEPAS technology using a QTF with f_0 of 30.72 kHz was demonstrated for the first time. A pigtailed, near infrared, continuous wave (CW), distributed feedback (DFB) diode laser emitting at 1.74 μm was employed as the excitation source. This sensor resulted in a 550 ppbv MDL for a 1 s data acquisition time. The ppb-level sensi-

tivity and robust design of QEPAS method makes it suitable for use in environmental monitoring and other applications.

2. Experimental setup

2.1. DFB diode laser characterization

The simulation of the HCl absorption line strength based on the HITRAN 08 database is shown in Fig. 1. From Fig. 1(a), we can determine that the strongest HCl absorption region of fundamental rotational-vibrational band is located in the 3.5 μm (1ν-band), which can be accessed using interband cascade lasers (ICLs) in the 3–4 μm wavelength region [16]. However, diode lasers with emission wavelength of <3 μm have several advantages, such as compactness, significant lower cost and higher optical power. Therefore, in this research, a 1.74 μm CW-DFB fiber-coupled diode laser (NEL Corp., Japan) in a 14-pin butterfly package that included a thermoelectric control (TEC) was employed as the excitation source to access the HCl 2ν overtone band located at 1.7 μm. Using the HITRAN data base we identified the 1742.38 nm (5739.27 cm⁻¹) absorption line as the strongest in the 1.7 μm spectral range (see

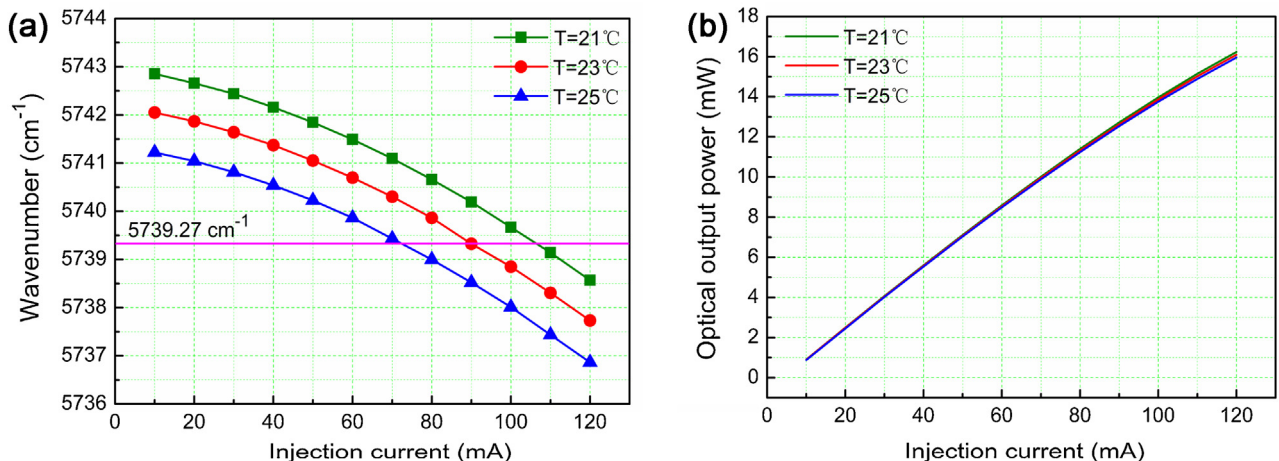


Fig. 2. 1.74 μm CW-DFB fiber-coupled diode laser output performance: (a) current tuning at different operating temperatures; (b) optical output power as a function of injection current.

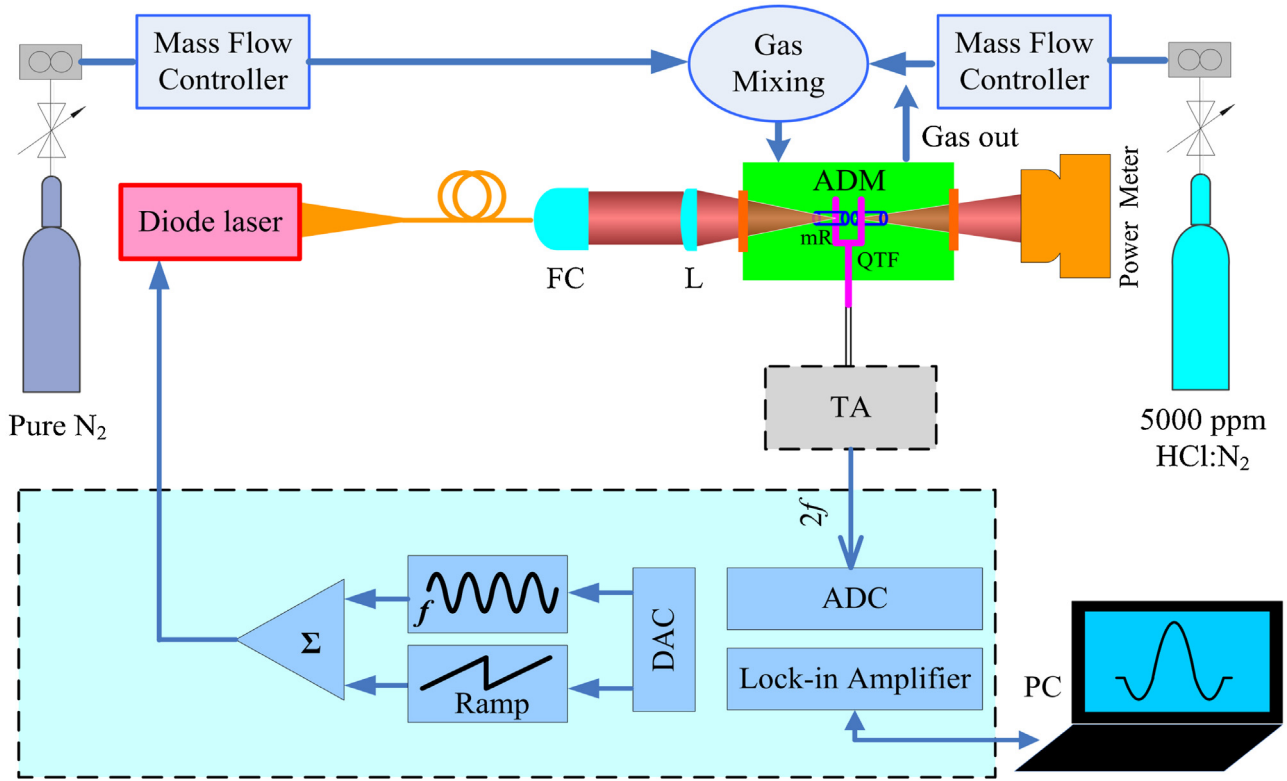


Fig. 3. Schematic configuration of a QEPAS system for HCl detection.

Fig. 1(b)) at a temperature of 296 K, standard atmospheric pressure and an optical path length of 1 cm for 5000 ppm HCl. This absorption line is free from spectral interference of other molecules. The absorption coefficient is $\sim 0.003 \text{ cm}^{-1}$ which is sufficient to provide a strong QEPAS signal.

The diode laser output performance was verified and is shown in **Fig. 2**. The experimentally determined temperature and current tuning coefficients of the laser were $-0.43 \text{ cm}^{-1}/^\circ\text{C}$ and $-0.039 \text{ cm}^{-1}/\text{mA}$, respectively. The maximum optical power emitted by the diode laser operating at temperature of 21°C and an injection current of 120 mA was $\sim 16.24 \text{ mW}$ (see **Fig. 2(b)**). The DFB diode laser can be current tuned to target the HCl absorption line of the first overtone at 1742.38 nm (5739.27 cm^{-1}), which is free from spectral interference of other molecules.

2.2. Sensor configuration

A schematic of the QEPAS based sensor platform is shown in **Fig. 3**. The laser beam was collimated by using a fiber collimator (FC) and subsequently focused between the QTF prongs inside acoustic detection module (ADM) by means of a plano-convex CaF_2 lens (L) with a 50 mm focal length. After passing through the ADM the laser beam was directed to an optical power meter (PS19Q, Coherent) and used for alignment verification of the QEPAS based sensor system. A QTF with f_0 of 30.72 kHz was employed as the acoustic transducer. The geometry of QTF is listed in **Table 1**. For comparison, a QTF with f_0 of 32.768 kHz is also listed in **Table 1**. Wavelength modulation spectroscopy (WMS) with 2nd harmonic detection [17]

was utilized for sensitive concentration measurements. Modulation of the laser current was performed by applying a sinusoidal dither to the direct current ramp of the diode laser at half of the QTF resonance frequency ($f = f_0/2 = 15.36 \text{ kHz}$). The piezoelectric signal generated by the QTF was detected by a low noise transimpedance amplifier (TA) with a $10 \text{ M}\Omega$ feedback resistor and converted into a voltage, which was transferred to a custom built control electronics unit (CEU). The CEU provides the following three functions: 1) measurement of the QTF parameters, i.e. the quality factor Q , dynamic resistance R , and resonant frequency f_0 ; 2) modulation of the laser current at the frequency $f = f_0/2$; and 3) measurement of the $2f$ component generated by the QTF. The HCl-QEPAS sensor performance was evaluated at different HCl concentrations. Two mass flow controllers with a mass flow uncertainty of 3% were used to dilute 5000 ppmv (parts in 10^6 by volume) HCl in nitrogen (N_2). The measurements were carried out at atmospheric pressure and room temperature ($\sim 20^\circ\text{C}$).

3. Experimental results and discussion

The HCl-QEPAS sensor performance using a basic QTF was evaluated first. A certified mixture of 5000 ppm HCl: N_2 was used. The impact of distance (L) between the laser beam and the top of QTF prongs on QEPAS signal level was investigated and the experimental results are shown in **Fig. 4**. An insert in **Fig. 4** displays the laser beam, the QTF and the parameter L. The modulation depth of laser wavelength was set to 0.16 cm^{-1} . The $2f$ HCl-QEPAS signal amplitude increased rapidly with L when it was $<0.6 \text{ mm}$. The peak region of the $2f$ signal amplitude appeared in the range of L from 0.6 mm to 1.3 mm. With a further increase of L, the signal amplitude decreased due to the more challenging QTF prong vibration when the acoustic wave source is at the bottom of the QTF prongs. In the following experiments, an optimum value of L of 1 mm was chosen to achieve the maximum QEPAS signal amplitude.

Table 1
Parameters of geometries for QTFs.

QTF with f_0 (kHz)	Length (mm)	Width (mm)	Thickness (mm)	Gap (mm)
30.72	3.9	0.62	0.36	0.32
32.768	3.6	0.6	0.36	0.3

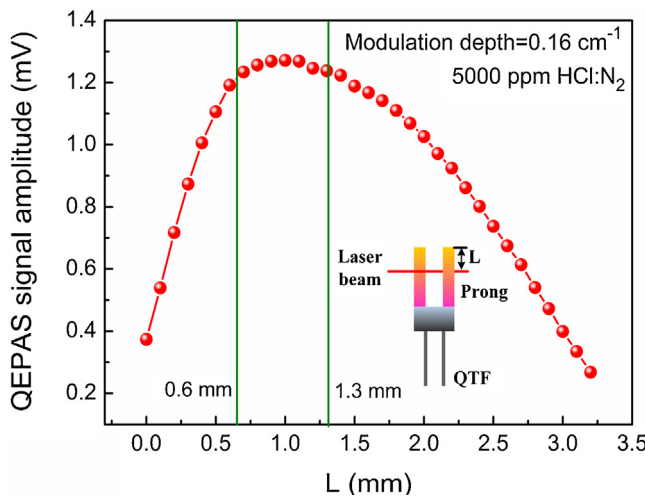


Fig. 4. HCl-QEPAS signal amplitude as a function of L at a modulation depth of 0.16 cm^{-1} .

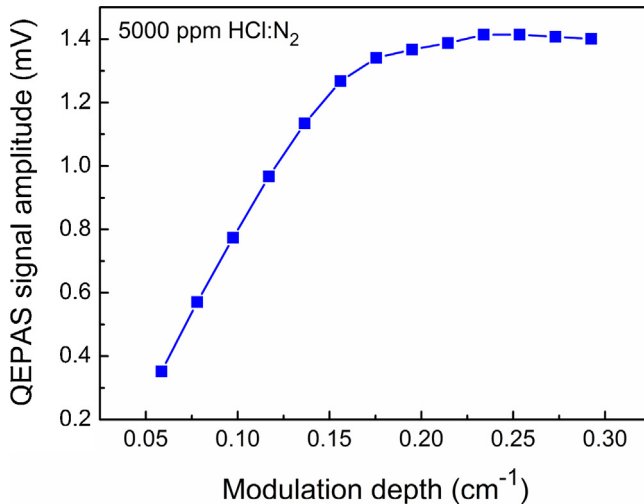


Fig. 5. HCl-QEPAS signal amplitude as a function of modulation depth for a 5000 ppm HCl:N₂ mixture.

The laser wavelength modulation depth was optimized in order to improve the $2f$ QEPAS signal amplitude. The dependence of the QEPAS signal amplitude as a function of the laser wavelength modulation depth is depicted in Fig. 5. The QEPAS signal amplitude increased with the modulation depth, but when the modulation depth was higher than 0.23 cm^{-1} , no further significant change was observed. Therefore, a modulation depth of 0.23 cm^{-1} was found to be optimum.

In our investigations, a QTF with a f_0 of 30.72 kHz was used. According to Eq. (1), a QTF with a low f_0 is advantageous to obtain a large QEPAS signal. Therefore, a comparison was made to confirm the advantages of using a QTF with f_0 of 30.72 kHz when compared to a standard QTF with a f_0 of 32.768 kHz . The experiments were carried out under the same conditions and the results are displayed in Fig. 6. We found that, compared to a QTF with f_0 of 32.768 kHz , the QEPAS signal increased 1.3 times when a QTF with f_0 of 30.72 kHz was used. Two aspects contributed to this QEPAS signal increase. One is a low f_0 of 30.72 kHz . The other is an increased Q factor. The Q factor for 32.768 kHz QTF was 7453 and that for 30.72 kHz QTF was 8996. The Q factor increased by 20% and according to Eq. (1) contributed to the QEPAS signal enhancement.

A significant enhancement of the QEPAS signal can be achieved when two metallic tubes acting as a micro-resonator (mR) are

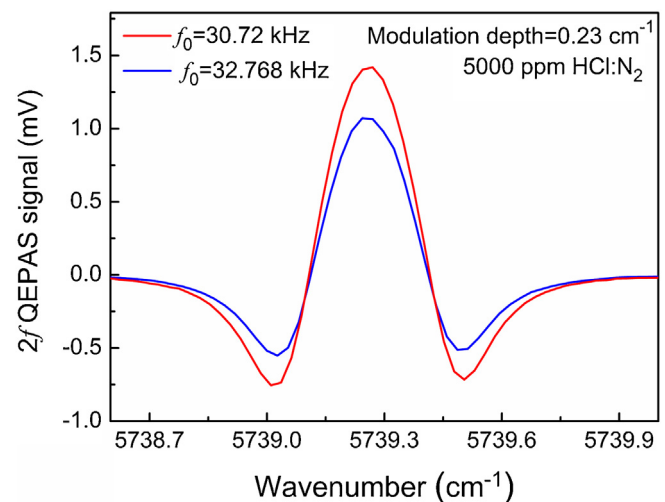


Fig. 6. $2f$ HCl-QEPAS signal for two QTFs with different f_0 of 30.72 kHz and 32.768 kHz for the same experimental conditions.

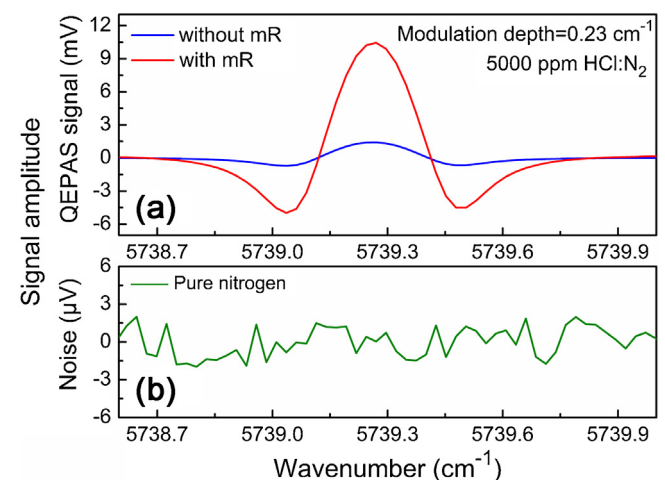


Fig. 7. Signal amplitude: (a) $2f$ HCl-QEPAS signal without and with mR obtained with a modulation depth of 0.23 cm^{-1} and using a QTF with f_0 of 30.72 kHz ; (b) pure N₂ for noise determination.

added to the QTF sensor architecture [18,19]. The optimum length L of metallic tubes should be in the range of $\lambda_s/4 < L < \lambda_s/2$, where λ_s is the sound wavelength. For a QTF with f_0 of 30.72 kHz , the optimum length should be $2.8 \text{ mm} < L < 5.5 \text{ mm}$. In this experiment, the length and inner diameter of stainless tubes were selected to be 4 mm and 0.5 mm respectively in order to compose the mR. The gaps between the QTF and mR tubes were chosen to be $25 \mu\text{m}$. The measured $2f$ QEPAS signals with and without mR at a modulation depth of 0.23 cm^{-1} is shown in Fig. 7(a). The QEPAS signal was enhanced 7.5-fold as a result of the addition of the two mR tubes. Fig. 7(b) depicts the background signal measured when the ADM was flushed with ultra high purity N₂. The background signal was $1.15 \mu\text{V}$ and is primarily determined by the fundamental thermal noise of the QTF. The QTF thermal noise can be expressed in terms of its root mean square (rms) voltage noise [12], and is shown in equation (2), where k_B is the Boltzmann constant, T is QTF temperature, R_g is the value of the feedback resistor used in a transimpedance amplifier located close to the ADM, R is the equivalent electrical parameter of resistance for the QTF when it is represented by an equivalent series resonant circuit. The measured equivalent resistance for the QTF was $643 \text{ k}\Omega$ and the calculated thermal noise was $1.41 \mu\text{V}$. Based on the data depicted in Fig. 7 the 1σ MDL of the

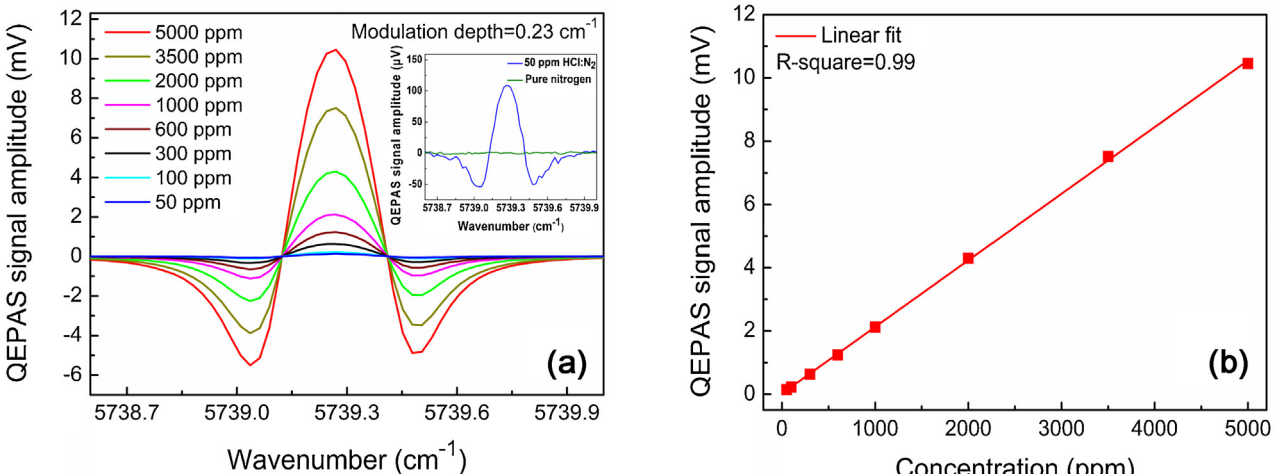


Fig. 8. (a) QEPAS signal amplitude at different HCl concentrations and a modulation depth of 0.23 cm⁻¹. Insert for 50 ppm HCl:N₂ and pure N₂ (b): QEPAS signals amplitude coming from (a) as a function of HCl concentrations.

HCl-QEPAS sensor is 550 ppbv for a 1 sec data acquisition time. The calculated normalized noise equivalent absorption coefficient (NNEA) is $1.76 \times 10^{-8} \text{ cm}^{-1} \text{ W}/\sqrt{\text{Hz}}$.

$$\sqrt{V_{rms}^2} = R_g \sqrt{\frac{4k_B T}{R}} \sqrt{\Delta f} \quad (2)$$

To verify the linear response of the QEPAS based HCl sensor platform a calibration mixture of 5000 ppm HCl:N₂ was diluted with dry N₂ down to 50 ppm HCl concentration levels (see Fig. 8(a)). The data acquisition time for these measurements was set to 1 sec. The measured QEPAS signal amplitude as a function of HCl concentrations are plotted in Fig. 8(b). The calculated R-square value, which represents how well the regression line approximates real data points, is equal to ~ 0.99 after a linear fitting procedure. This implies that the sensor system exhibits an excellent linearity response of the monitored HCl concentration levels. Based on the data depicted in the insert of Fig. 8(a), a 1σ MDL of 526 ppbv for the HCl-QEPAS sensor was achieved. The minor difference of MDL obtained from Fig. 7 and Fig. 8 resulted from the dilution process.

4. Conclusions

In conclusion, a sensitive QEPAS based HCl sensor using a QTF with f_0 of 30.72 kHz was demonstrated. A pigtailed, near infrared, CW, TEC, DFB diode laser emitting at 1.74 μm was employed as the laser excitation source. Wavelength modulation spectroscopy and a 2nd harmonic detection technique were used to reduce the sensor background noise and simplify data processing. A significant signal enhancement of 7.5 times was obtained when two mR were added to the QTF sensor architecture. For the HCl sensor system operating at atmospheric pressure, a 550 ppbv MDL at 5739.27 cm⁻¹ was achieved when the modulation depth and data acquisition time were set to 0.23 cm⁻¹ and 1 s, respectively. Furthermore, the detection limit can be further improved when a QTF with a lower f_0 and multiple QTFs are adopted [20]. With a detection sensitivity at ppb concentration levels the reported HCl QEPAS based sensor is suitable for applications in environmental monitoring, atmospheric chemistry and industrial chemical analysis.

Acknowledgments

This work was supported by the National Natural Science Foundation of China (Grant No. 61505041), the Natural Science Foundation of Heilongjiang Province of China (Grant No.

F2015011), the General Financial Grant from the China Postdoctoral Science Foundation (Grant No. 2014M560262), the Special Financial Grant from the China Postdoctoral Science Foundation (Grant No. 2015T80350), the Special Financial Grant from the Heilongjiang Province Postdoctoral Foundation (Grant No. LBH-TZ0602), the Postdoctoral Fund of Heilongjiang Province (Grant No. LBH-Z14074), the Fundamental Research Funds for the Central Universities (Grant No. HIT.NSRIF.2015044), and the National Key Scientific Instrument and Equipment Development Projects of China (Grant No. 2012YQ040164). Frank K. Tittel gratefully acknowledges the financial support from the US National Science Foundation ERC MIRTHER award and a grant C-0586 from the Welch Foundation.

References

- [1] L. Wang, R.V. Kumar, Thick film miniaturized HCl gas sensor, *Sens. Actuators B* 98 (2004) 196–203.
- [2] Z.S. Li, Z.W. Sun, B. Li, M. Alden, M. Forsth, Spatially resolved trace detection of HCl in flames with mid-infrared polarization spectroscopy, *Opt. Lett.* 33 (16) (2008) 1836–1838.
- [3] Y.B. Huang, Y.A. Yang, G.X. He, S. Hashimoto, R.J. Gordon, State resolved translational energy distributions of Cl and HCl in the ultraviolet photodissociation of chloroethylenes, *J. Chem. Phys.* 103 (1995) 5476–5487.
- [4] S. Kim, P. Klimecky, J.B. Jeffries, F.L. Terry, R.K. Hanson, In situ measurements of HCl during plasma etching of poly-silicon using a diode laser absorption sensor, *Meas. Sci. Technol.* 14 (2003) 1662–1670.
- [5] H. Supriyatno, M. Yamashita, K. Nakagawab, Y. Sadaoka, Optochemical sensor for HCl gas based on tetraphenylporphyrin dispersed in styrene-acrylate copolymers: effects of glass transition temperature of matrix on HCl detection, *Sens. Actuators B* 85 (2002) 197–204.
- [6] P. Ortwein, W. Woiwode, S. Fleck, M. Eberhard, T. Kolb, S. Wagner, M. Gisi, V. Ebert, Absolute diode laser-based in situ detection of HCl in gasification processes, *Exp. Fluids* 49 (2010) 961–968.
- [7] J. Li, U. Parchatka, R. Königstedt, H. Fischer, Real-time measurements of atmospheric CO using a continuous-wave room temperature quantum cascade laser based spectrometer, *Opt. Express* 20 (2012) 7590–7601.
- [8] Y.Y. Tang, W.Q. Liu, R.F. Kan, J.G. Liu, Y.B. He, Y.J. Zhang, Z.Y. Xu, J. Ruan, H. Geng, Measurements of NO and CO in Shanghai urban atmosphere by using quantum cascade lasers, *Opt. Express* 19 (2011) 20224–20232.
- [9] J.B. McManus, M.S. Zahniser, D.D. Nelson, Dual quantum cascade laser trace gas instrument with astigmatic Herriott cell at high pass number, *Appl. Opt.* 50 (2011) A74–A85.
- [10] A. Elia, P.M. Lugarà, C. di Franco, V. Spagnolo, Photoacoustic techniques for trace gas sensing based on semiconductor laser sources, *Sensors* 9 (2009) 9616–9628.
- [11] A.A. Kosterev, Y.A. Bakirkin, R.F. Curl, F.K. Tittel, Quartz-enhanced photoacoustic spectroscopy, *Opt. Lett.* 27 (2002) 1902–1904.
- [12] A.A. Kosterev, F.K. Tittel, D.V. Serebryakov, A.L. Malinovsky, I.V. Morozov, Applications of quartz tuning forks in spectroscopic gas sensing, *Rev. Sci. Instrum.* 76 (2005) 043105.

- [13] S. Borri, P. Patimisco, A. Sampaolo, M.S. Vitiello, H.E. Beere, D.A. Ritchie, G. Scamarcio, V. Spagnolo, Terahertz quartz enhanced photo-acoustic sensor, *Appl. Phys. Lett.* 103 (2013) 021105.
- [14] P. Patimisco, S. Borri, A. Sampaolo, H.E. Beere, D.A. Ritchie, M.S. Vitiello, G. Scamarcio, V. Spagnolo, Quartz enhanced photo-acoustic gas sensor based on custom tuning fork and terahertz quantum cascade laser, *Analyst* 139 (2014) 2079–2087.
- [15] H.P. Wu, A. Sampaolo, L. Dong, P. Patimisco, X.L. Liu, H.D. Zheng, X.K. Yin, W.G. Ma, L. Zhang, W.B. Yin, V. Spagnolo, S.T. Jia, F.K. Tittel, Quartz enhanced photoacoustic H₂S gas sensor based on a fiber-amplifier source and a custom tuning fork with large prong spacing, *Appl. Phys. Lett.* 107 (2015) 111104.
- [16] W. Ren, L.Q. Luo, F.K. Tittel, Sensitive detection of formaldehyde using an interbandcascade laser near 3.6 μm, *Sens. Actuators B* 221 (2015) 1062–1068.
- [17] Y.F. Ma, R. Lewicki, M. Razeghi, F.K. Tittel, QEPAS based ppb-level detection of CO and N₂O using a high power CW DFB-QCL, *Opt. Express* 21 (1) (2013) 1008–1019.
- [18] L. Dong, V. Spagnolo, R. Lewicki, F.K. Tittel, Ppb-level detection of nitric oxide using an external cavity quantum cascade laser based QEPAS sensor, *Opt. Express* 19 (24) (2011) 24037–24045.
- [19] K. Liu, J. Li, L. Wang, T. Tan, W. Zhang, X.M. Gao, W.D. Chen, F.K. Tittel, Trace gas sensor based on quartz tuning fork enhanced laser photoacoustic spectroscopy, *Appl. Phys. B* 94 (2009) 527–533.
- [20] Y.F. Ma, X. Yu, G. Yu, X.D. Li, J.B. Zhang, D.Y. Chen, R. Sun, F.K. Tittel, Multi-quartz-enhanced photoacoustic spectroscopy, *Appl. Phys. Lett.* 107 (2015) 021106.

Biographies

Yufei Ma received his Ph.D. degree in physical electronics from Harbin Institute of Technology, China, in 2013. From September 2010 to September 2011, he spent as a visiting scholar at Rice University, USA. Currently, he is a lecturer at the Harbin Institute of Technology, China. His research interests include optical sensors, trace gas detection, laser spectroscopy and optoelectronics.

Ying He received his B.S. degree in optoelectronic material and device from Harbin Engineering University, China, in 2015. He is now pursuing a M.S. degree of physical electronics from the Harbin Institute of Technology. His research interests include photoacoustic spectroscopy and optoelectronics techniques.

Xin Yu received her Ph.D. degree in physical electronics from Harbin Institute of Technology, China, in 2002. Now she is a professor at the Harbin Institute of Technology. Her research interests include laser detection, laser diagnostics, solid-state laser, laser ignition and optical sensors.

Rui Sun received his Ph.D. degree in thermal engineering from Harbin Institute of Technology in 1998. He is currently a professor in the College of Energy Science Engineering of the Harbin Institute of Technology. His research interests include clean coal combustion, alternative fuels (as biomass, waste etc.), optical diagnostics and laser spectroscopy.

Frank K. Tittel received his B.S. degree in 1955 and the Ph.D. degree in 1959 from Oxford University. He is the J.S. Abercrombie professor in the Department of Electrical Engineering at Rice University, Houston, TX USA. Professor Frank Tittel has been involved in many innovative developments in quantum electronics and laser technology since the discovery of the laser in 1960, with applications ranging from laser spectroscopy to environmental monitoring. The most recent designs utilize novel mid-infrared quantum cascade and interband lasers to achieve compact, robust instrumentation that can be deployed for field applications, such as by the US Environmental Protection Agency (EPA) for urban formaldehyde monitoring, methane and ethane detection funded by the US Department of Energy ARPA-E MONITOR program and by the US National Institute of Health for non-invasive NO and CO detection based on biomedical systems.